Am J Cancer Res 2025;15(10):4320-4329
www.ajcr.us /ISSN:2156-6976/ajcr0166549

Original Article

The CXCR1 as a putative marker for cancer stem cell-like phenotypes in chemotherapy-resistant pancreatic ductal adenocarcinoma

Caitlin Molczyk, Reegan Sturgeon, Elizabeth Thomas, Rakesh K Singh

Department of Pathology, Microbiology, and Immunology, 985950 Nebraska Medical Center, Omaha, NE 68198-5900, USA

Received June 3, 2025; Accepted September 4, 2025; Epub October 15, 2025; Published October 30, 2025

Abstract: Cancer stem cells (CSCs) are a rare but critical subpopulation in pancreatic ductal adenocarcinoma (PDAC), contributing to therapy resistance and disease relapse. The CXCR1 signaling axis has been implicated in CSC maintenance across multiple cancers. We investigated the role of CXCR1 in CSC-like phenotypes in PDAC by analyzing its expression, along with established CSC markers, in chemotherapy-resistant (GemR) and parental PDAC cell lines under various treatment conditions. GemR cells exhibited elevated levels of CXCR1, its ligand CXCL6, and CSC markers compared to parental lines. Gemcitabine treatment increased the expression of CXCR1 and CSC-associated markers in parental cells, suggesting therapy-induced enrichment of CSC-like populations. Additionally, GemR cells had a higher frequency of $CD44^+/CXCR1^+$ cells. In parental cells, gemcitabine also induced markers of epithelial-to-mesenchymal transition (EMT), a phenotype associated with CSC plasticity. Combination treatment with gemcitabine and Navarixin, a CXCR1 inhibitor, significantly reduced expression of CXCR1, CXCL6, and CSC/EMT markers in vitro. *In vivo*, tumors treated with the combination therapy showed markedly lower CXCR1 and CXCL6 expression than other treatment groups. These findings indicate that the CXCR1 axis supports CSC maintenance in PDAC, and that co-targeting CSC and non-CSC populations may improve therapeutic outcomes.

Keywords: CXCR1, cancer stem cells, PDAC, therapy resistance

Introduction

Pancreatic cancer is the fourth leading cause of cancer-related deaths. The survivorship of patients diagnosed with pancreatic cancer is dismal, with a mere 13% survival rate after five years of diagnosis [1]. The most common pancreatic cancer is pancreatic ductal adenocarcinoma (PDAC), making up 95% of pancreatic cancer cases. PDAC is an incredibly aggressive form of pancreatic cancer with high mortality due to its ability to resist chemotherapy and metastasize. These highly aggressive characteristics of PDAC can be attributed to a subpopulation of cells known as CSCs. CSCs are considered initiators of the tumor [2]. What separates these cells from the bulk tumor is that they have characteristics of stem cells, such as slow cell cycling, being capable of self-renewal, and leading to clonal repopulation [2-4]. CSCs have also shown a higher resistance to chemotherapy, allowing them to overcome treatment and maintain tumor growth [5].

These attributes make PDAC CSCs an appealing therapeutic target; however, they are elusive, constituting less than 1-2% of the tumor [6]. Much of the previous research investigating CSCs relies on cell markers to locate them. For PDAC CSCs, several known markers include CXCR4, CD133, CD24, CD44, and the internal SOX2 and NANOG transcription factors, which are used to evaluate stemness [5-7]. However, most of these markers are solely for identifying CSCs and are not used as therapeutic targets. A promising marker of interest that can be therapeutically inhibited is CXCR1. This C-X-C receptor is most known for its role in inflammatory responses. Upon binding its ligands, CXCL6 and CXCL8, CXCR1 facilitates chemotaxis, promotes angiogenesis, and enhances bacterial immune system response under normal conditions [8].

https://doi.org/10.62347/YLHF5834

Table 1. Antibodies used in these studies

	Primary Antibody	Marker	Source	Catalog No.	Dilution
1	Anti-CXCR1	CXCR1	Novus Biologicals	IMG-334	1:100
2	Anti-CD44	CSC marker	Cell Signaling, MA, USA	mAB-37259	1:300
3	Anti-CD133 (PROM1)	CSC marker	Invitrogen	MA1-219	1:100
4	Biotinylated Anti-Rabbit IgG		Vector laboratories, Inc. Burlingame, CA, USA	BA-1000	1:500
5	FITC labeled goat anti-rabbit IgG		Vector laboratories, Inc. Burlingame, CA, USA	FI-1000	1:500
6	Texas Red Avidin D		Vector laboratories, Inc. Burlingame, CA, USA	A-2006	1:50

In a pathologic condition, the CXCR1 axis elicits a response that promotes metastasis/migration [9-13], invasion [14-16], neovascularization [9, 13, 15, 17], increased proliferation [9, 13, 18], and chemotherapy resistance [10-12, 19]. In a recent review, we described several solid tumors with CXCR1 as a potential CSC-like marker [20]. By utilizing a CXCR1 inhibitor called repertaxin in triple negative breast cancer (TNBC), Ginestier et al. demonstrated that this decreased the CSCs' ability to form tumorspheres, invade, and metastasize [10]. In PDAC, Chen et al. showed similar results in PDAC CSCs by neutralizing CXCL8 with a CXCL8 antibody. Both results suggest that CXCR1 plays an essential role in tumorigenesis, invasion, and metastasis [11]. Further exploration of this pathway in PDAC is crucial for developing CSC-targeted therapies.

In the research presented here, we used two cell lines, CD18/HPAF (CD18) and T3M4, to examine the role of CXCR1 in PDAC. Using the parental cell lines, we generated chemotherapy-resistant cell lines. We compared the CXCR1 expression in each of the parental and chemotherapy-resistant cell lines. The cell lines were treated with Gemcitabine (Gem) and Navarixin (Nav), a CXCR1/2 inhibitor. qRT-PCR, ELISA, flow cytometry, and immunofluorescence were used to compare the cell lines. We used commonly known CSC and EMT markers to evaluate the expression of CSC-like characteristics between the groups. Our data suggest that CXCR1 is a potential avenue to explore targeting for CSC-like cells in the PDAC TME.

Materials and methods

Cell lines and reagent

All the cell lines were tested for mycoplasma using MycoAlert Plus Mycoplasma Detection kit (Lonza, Rockland, ME). Cell lines were authenticated by the Human DNA Identification Laboratory, UNMC, Omaha, NE, through short tandem repeat (STR) tests.

PDAC human cell lines T3M4 and CD18 were maintained in Dulbecco's Modified Eagle Medium (DMEM), supplemented with 5% fetal bovine serum (FBS), L-glutamine, 10X vitamin solution, and gentamycin.

To develop CD18 and T3M4 Gemcitabine-resistant (GemR) cell lines, we treated the cell lines with increasing concentrations of the chemotherapy for 3-6 months. These cells were verified to be resistant to the chemotherapy with MTT assays with increasing concentrations of the chemotherapy and compared to the parent cell line response.

CXCR1/2 inhibitor SCH-527123 (Navarixin) was obtained from Schering-Plough Research Institute. These were reconstituted to the manufacturer's recommendations using the appropriate reagents. Gem (Sagent and Meathial, NDC: 25021-234-10 and 71288-113-10) was obtained through the pharmacy at Nebraska Medicine. All the antibodies used for the present study are listed in **Table 1**.

mRNA analysis

Total RNA was isolated using Trizol using the manufacturer's protocol. Reverse transcription was performed with 1-5 µg RNA using Applied Sciences Reverse Transcription supermix for qRT-PCR. Quantitative real-time PCR (qRT-PCR) reactions were performed using iTaq Universal SYBR Green super mix (bio-rad) using the QuantStudio 3 System. Primers used for these studies are listed in **Table 2**. To normalize the qRT-PCR values, a housekeeping gene control (ribosomal protein large 13A (RPL13)) was used to normalize the C_t value for the relative expres-

Table 2. Primers used in these studies

	Gene of interest	Sequences forward and reverse	Melting Temperature (°C)	Annealing Temperature (°C)
1	huCXCR1	5'-GAGCCCCGAATCTGACATTA-3' 5'-GCAGACACTGCAACACACCT-3'	73	59
3	huCXCL8	5'-ACATACTCCAAACCTTTCCACCC-3' 5'-CAACCCTCTGCACCCAGTTTTC-3'	63	59
4	huCXCL6	5'-AGAGCTGCGTTGCACTTGTT-3' 5'-GCAGTTTACCAATCGTTTTGGGG-3'	62	58
7	CD44	5'-CTGCCGCTTTGCAGGTGTA-3' 5'-CATTGTGGGCAAGGTGCTATT-3'	57	53
9	SNAIL	5'-TTTACCTTCCAGCAGCCCTA-3' 5'-CCCACTGTCCTCATCTGACA-3'	62	58
10	SLUG	5'-CGAACTGGACACACATACAGTG-3' 5'-CTGAGGATCTCTGGTTGTGGT-3'	56	52
16	NANOG	5'-CCCCAGCCTTTACTCTTCCTA-3' 5'-CCAGGTTGAATTGTTCCAGGTC-3'	56	52
17	Oct-4	5'-GGGAGATTGATAACTGGTGTGTT-3' 5'-GTGTATATCCCAGGGTGATCCTC-3'	56	52
18	RPL13	5'-ACCGTCTCAAGGTGTTTGACG-3' 5'-GTACTTCCAGCCAACCTCGTG-3'	61	57

sion of the gene of interest by [ΔC_T = RPL13 C_t - Target gene C_t]. The normalized ΔC_t value was then taken $2^{-\Delta CT}$ to obtain the relative expression. A melting curve analysis was performed to check the amplified product's specificity.

Animal studies

The study was approved by the University of Nebraska Medical Center Institutional Animal Care and Use Committee (IACUC). We kept the mice under specific pathogen-free conditions throughout the study and performed all procedures per institutional guidelines. The animal model and treatment schedule used for this experiment are shown in **Figure 4**. 6-8-week-old immunodeficient (nude) mice were orthotopically injected with CD18 or CD18 GemR cells (5×10^5 cells in 30 uL HBSS). Seven days post-inoculation, the mice were divided into four treatment groups: control, Navarixin (5 mg/kg), Gem (25 mg/kg), and combination. The drug doses were optimal based on the previous observation in the laboratory. They were treated for 28 days (CD18 GemR). The tumors were then resected and processed for histological and staining analysis.

Immunofluorescence analysis

To explore the expression of various tissue markers, we performed or immunofluorescent (IF) staining. First, 4-5 μm thick, formalin-fixed, paraffin-embedded tissue sections were prewarmed at 65°C for 2 hours or overnight on the slide warmer and then deparaffinized with graded xylene. The slides were rehydrated through descending concentrations of ethanol in water. Afterward, antigen retrieval was performed using sodium citrate buffer (pH = 6.0) and heating in the laboratory microwave for 10 minutes. Endogenous peroxidase was blocked by incubating with 3% hydrogen peroxide for 5 minutes. After blocking non-specific binding by incubating with serum, slides were probed with respective primary antibodies (**Table 2**) and incubated overnight at 4°C. The following day, slides were washed and incubated with appropriate secondary antibodies. Finally, the slides were mounted with Aquamount (Epredia, Breda, Netherlands). At least two independent observers evaluated IF staining. For quantitative evaluation, in each tissue section of the slides, positive cells were counted in five areas with significant staining at 200X magnification. Then their average is used for plotting the graph. All the above analyses were done, and the representative photomicrographs were captured with a Nikon Eclipse E800 microscope and its NIS-Elements BR 5.11.00 software (Nikon, Melville, NY).

Flow cytometric analysis

CD18 and CD18 GemR cells were plated into 100 mm × 15 mm petri dishes, 1×10^6 cells

per dish. They were split into treatment groups: control, gem, nav, and combination, using IC_{50} concentrations of drugs and treated for 72 hours. These cells were then trypsinized, counted, and added to 5-mL tubes used for flow cytometry, so there were 1×10^6 cells per tube in 1 mL of media. These tubes were labeled as test tubes. Control tubes were also made. In the control tube, we added 10 µL of DEAB. We added 2 µL of the ALDEFLUOR reagent to the test tube, took out 500 uL, and placed it in the tube, vortexing quickly. These were incubated for 60 minutes at 37°C. Then they were spun down at 250×g for 5 minutes, resuspended in ALDEFLUOR assay buffer, and stored on ice. Ten minutes before using the flow sorter, we added 10 µL propidium iodide for viability. The flow cytometry was performed in the Flow Cytometry Core Facility at the University of Nebraska Medical Center. We used LSRII and LSRII G to sort the cells. The data were analyzed using BC FACSDiva and Flow Jo.

Statistical analysis

The statistical analysis for all experiments was performed using the Prism 7 (GraphPad) software. The sample number and statistical method are indicated in the chapters. Statistical significance was defined at $P \leq 0.05$. The error bars on the figures represent the standard error of the mean. The analyses used when appropriate included the two-tailed Student's t-test, ANOVA, and Posthoc comparisons using Mann-Whitney tests with a Bonferroni adjustment.

Results

Higher expression of the CXCR1, its ligand CXCL6, and increased CSC markers in therapy-resistant cells

In our primary evaluation of the CXCR1 axis and its association with a CSC-like phenotype, we pursued analysis of the GemR and parental cell lines. There is a previously reported association between $CXCR1^+$ cells and CSC-like phenotype in TNBC [10]. Our investigation showed increased CXCR1 expression in the CD18-GemR and T3M-GemR cell lines as compared to their respective parental cells (**Figure 1A**). Similarly, we observed an increased expression of CXCL6 (a ligand for CXCR1) in CD18-GemR and T3M4-GemR cells (**Figure 1A**).

Next, we evaluated the expression of known CSC-associated markers. The CSC marker CD44 was increased in CD18-GemR and T3M4-GemR cells as compared to parental cells (**Figure 1A**). The expression of CSC transcription factors OCT4 and NANOG was also increased in the T3M4-GemR cell line as compared to parental cells (**Figure 1A**). EMT and CSCs are thought to be highly correlated, so we also explored SLUG expression as an EMT transcription factor and demonstrated it was increased in the GemR cell line (**Figure 1A**). Together these data suggest higher expression of CXCR1, its ligands CXCL6 and CSC-associated markers in gemcitabine resistant cells.

Gemcitabine treatment modulates the expression of the CXCR1 axis and CSC markers

Previously found in our lab and others, chemotherapy increases the expression of CSC-associated markers [21, 22]. Here, we examined whether gemcitabine treatments modulate the expression of CXCR1 and CSC-associated markers in PDAC. We found an increase in the expression of the CXCR1, CXCL6, and CD44 and OCT4 following gemcitabine treatment (**Figure 1B**). The other CSC transcription factor NANOG, showed an increasing trend in its expression, however, SLUG showed a decrease following gemcitabine treatment (**Figure 1B**).

Gemcitabine-resistant cell lines displayed treatment-dependent modulation of the CSC markers

In exploring how the CXCR1 antagonist affects the GemR cell lines, we treated the T3M4-GemR cells. We found increased CXCR1 and CXCL6 expression when treated with Gem in the T3M4 GemR cell line (**Figure 2**). There was a differential increase in the expression of OCT4, NANOG, and SLUG in gemcitabine resistant PDAC cells when treated with chemotherapy (**Figure 2**).

Navarixin treatment showed no significant changes in expression between the control and gemcitabine treatment. The combined treatment of Gemcitabine and Navarixin decreased the expression of all the markers compared with the gemcitabine alone treatment, even in comparison to the control treatment (**Figure 2**).

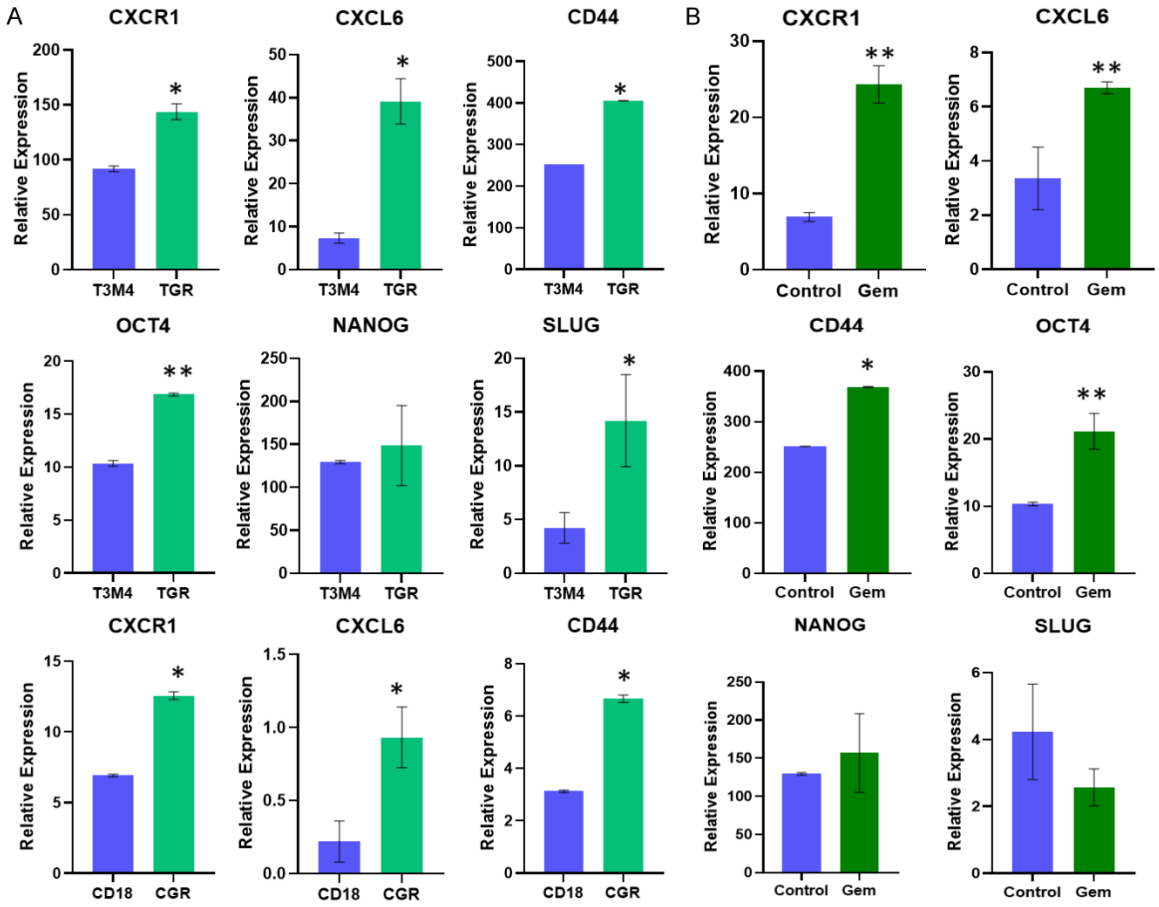

Figure 1. Expression of the CXCR1, CXCL6, and CSC-associated markers. A. The mRNA expression of CXCR1, CXCL6, CD44, OCT4, NANOG, and SLUG in parent and derived GemR cell lines. B. The mRNA expression of CXCR1, CXCL6, OCT4, NANOG, and SLUG in T3M cells treated with Gemcitabine for 72 hours. The data presented is a representative of three experiments done in triplicate. *P<0.05, **P<0.01, ***P<0.001.

Higher co-localization of CXCR1 and CSC markers in the GemR cell lines

We found higher expression of CD44 alone in the T3M4-GemR and CD18-GemR cell lines (**Figure 3A**). There is also a higher expression of the CXCR1 in the GemR cell lines (**Figure 3A**). Interestingly, when the images were overlapped, we found they co-localized and were more highly expressed in the GemR cell lines as compared to parental cells (**Figure 3A**).

In the continued effort to evaluate CXCR1 as a CSC marker in PDAC, we also wanted to analyze the ALDH-expressing populations using flow cytometry. We observed an increase in the number of ALDH$^+$ cells in the CD18-GemR cell line (**Figure 3B**). The CD18-GemR cell line had increased frequency of the ALDH$^+$ cells when treated with Gem; and when treated with the combination, there was a decrease in ALDH$^+$ cells (**Figure 3B**). Although there was no significant change between the Navarixin and control treatments, there was a difference between the combination (Nav + Gem) and Gemcitabine treatments (**Figure 3B**). The difference between the combination (Nav + Gem) and Gem treatment suggest that adding Navarixin with Gemcitabine can decrease the number of ALDH$^+$ GemR tumor cells.

Decreased CXCR1 and CXCL6 expression in combination therapy-treated PDAC tumors

The *in vivo* experiment involved CD18 GemR cells injected orthotopically in nu/nu mice. Seven days later, treatment started for their respective groups for 14 days. When the mice were sacrificed, the tumors were isolated and analyzed (**Figure 4**). There was a drastic de-

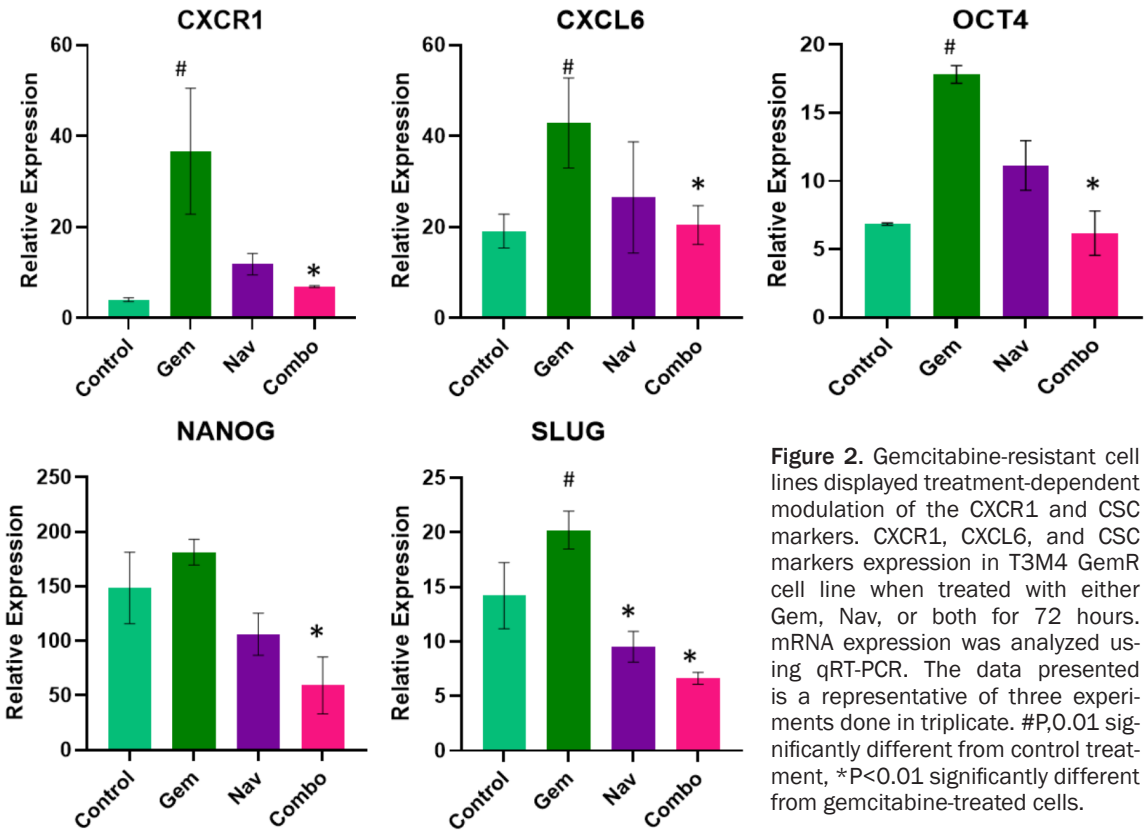

Figure 2. Gemcitabine-resistant cell lines displayed treatment-dependent modulation of the CXCR1 and CSC markers. CXCR1, CXCL6, and CSC markers expression in T3M4 GemR cell line when treated with either Gem, Nav, or both for 72 hours. mRNA expression was analyzed using qRT-PCR. The data presented is a representative of three experiments done in triplicate. #P,0.01 significantly different from control treatment, *P<0.01 significantly different from gemcitabine-treated cells.

crease in the expression of CXCR1 in all treatment groups compared with the control (**Figure 4C**). The CXCL6 expression increased with gem treatment and drastically decreased when treated with a combination (Nav + Gem) (**Figure 4D**), even though Nav treatment did not alter the expression.

Discussion

The CSC phenotype is undoubtedly a tricky one to identify and treat. Previous data support the role of CXCR1 as a marker and therapeutic target for CSCs in TNBC [10], which is the most difficult breast cancer to treat and continues to have the worst outcomes [23]. Though less common than breast cancer, PDAC is the fourth leading cause of cancer-related deaths and continues to have worse results, considering the low incidence with high mortality of the disease. The ability of this tumor to have such dynamic growth in such volatile circumstances makes us wonder how it is surviving and metastasizing. A cell type that would thrive under such circumstances is a CSC. These dynamic cells can become dormant under unsuitable conditions, self-renew, and regenerate the tumor mass. They are also known to metastasize as well as resist chemotherapy.

The CXCR1 axis is closely related to the CXCR2 axis, though it only binds two ligands compared to the seven of the latter. Though both appear to have similar roles in the immune and wound healing response [24-32], they have been evolutionarily conserved [33, 34], suggesting either an extremely important pathway duplication or an essential role for their downstream functions. In this study, we assessed the role of CXCR1 as a CSC marker in PDAC.

Previously reported by Chen et al., the CXCR1 antibody targeting decreased *in vitro* PDAC colony-forming in the presence of exogenous CXCL8. The specificity of CXCR1 being targeted and decreasing growth led us to explore further. Our studies showed an increased expression of CXCR1 receptor and its ligand, CXCL6, in gemcitabine-resistant PDAC cells. Moreover, we observed trends of increasing expression of the CSC and EMT markers comparing the GemR cell lines to the parental, suggesting that the resistant cells express higher CXCR1 and CSC-associated markers.

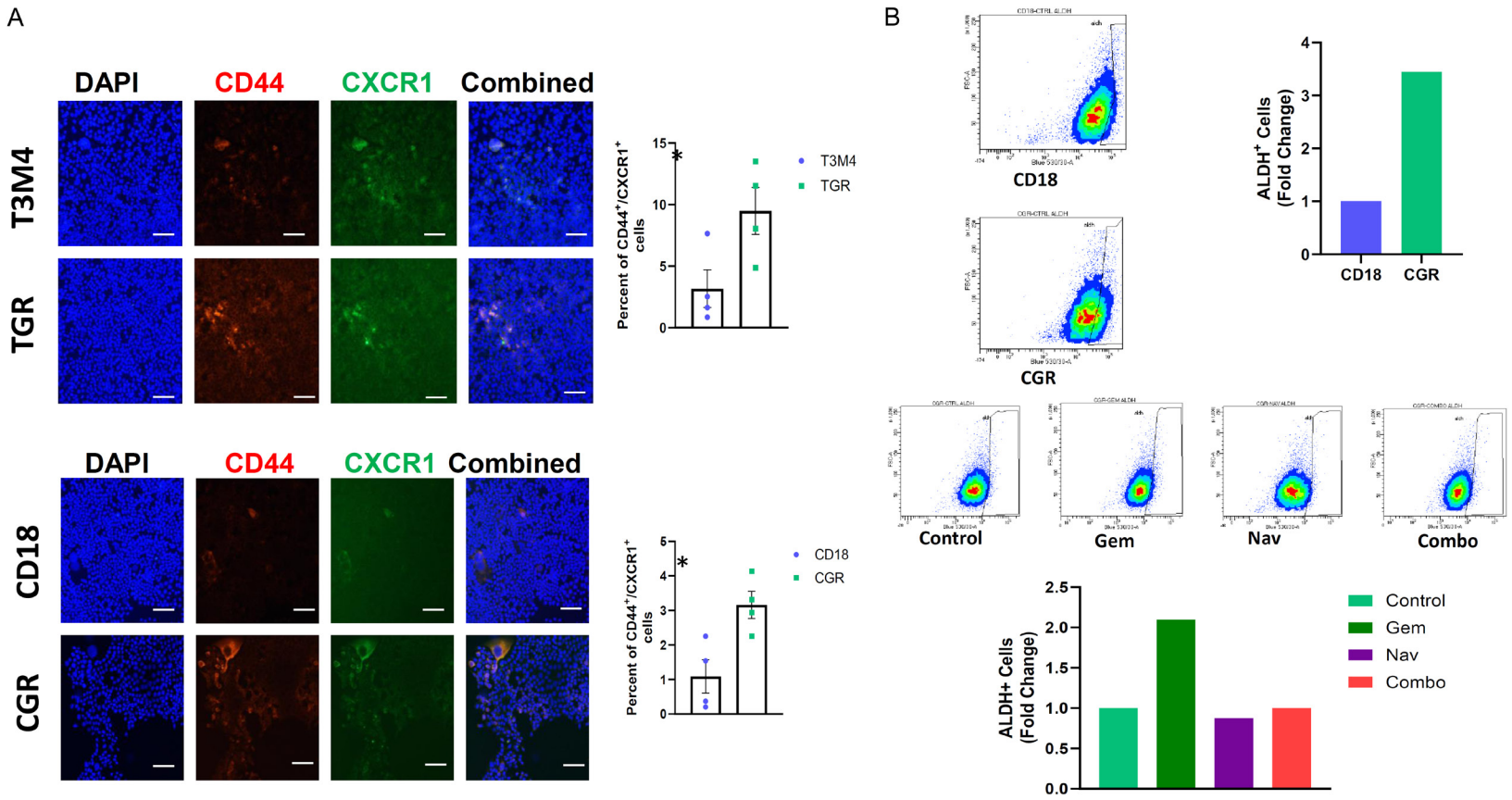

Figure 3. Differential expression of CSC markers on parent and resistant cell lines. A. The parent and GemR cell lines (TGR and CGR) were stained for DAPI, CD44, and CXCR1 and combined. The comparison of $CD44^+/CXCR1^+$ between the parent and resistant cell lines, where both T3M4 GemR (TGR) and CD18 GemR (CGR) demonstrate an increase compared to the parental cell lines. B. CD18 parent and GemR cell lines evaluated for $ALDH^+$ expression. A graphical representation of the fold change of $ALDH^+$ populations in CD18 versus the derived CD18 GemR cell line are presented. $ALDH^+$ populations in the CD18 GemR cell line: control, gem, nav, and combination treatments were examined by flow cytometry analysis. The graphical representation of the fold change in the $ALDH^+$ populations with treatment is presented. The data presented is a representative of two experiments done in duplicate. The scale bar represents 50 uM.

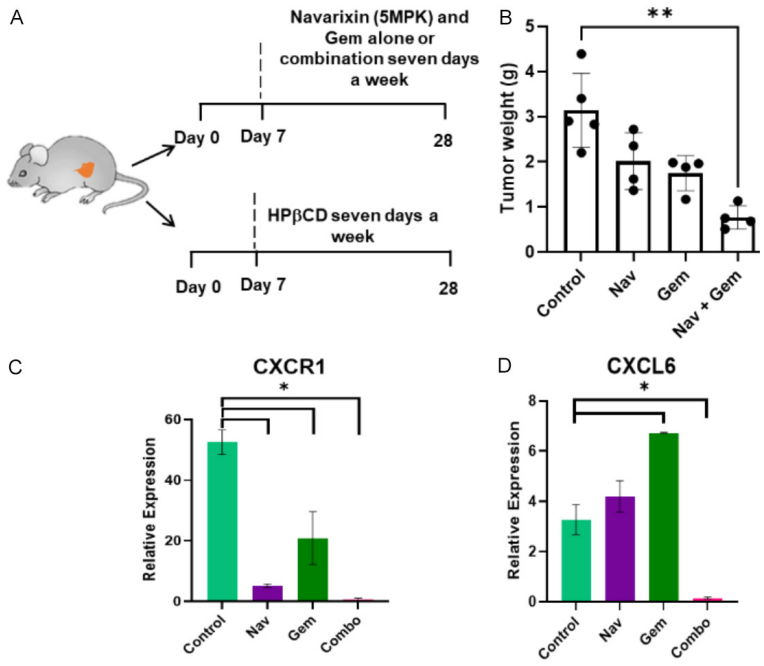

Figure 4. Decreased CXCR1 and CXCL6 expression in combination therapy-treated PDAC tumors. *In vivo* experiment with orthotopic injection of the CD18 GemR cell line into nude mice for evaluation of the CXCR1 axis. The outline of the mouse experiment is shown in (A, B). The size and weights of the tumors from the animal treatment groups (n = 5 mice per group). The expression of CXCR1 (C) and CXCL6 (D) from the *in vivo* experiment with the experimental treatment groups: control, gemcitabine (Gem), Navarixin (Nav), and combination (Gem + Nav). The data presented is a representative of two experiments done. A significant decrease in both markers is observed when treated in combination. *P<0.05.

Our data demonstrate that chemotherapy enhanced the expression of CXCR1 and CSC, and EMT markers. There have been reports from our laboratory and others suggesting that chemotherapy induces plasticity of cancer cells and increases CSC-like capabilities [21, 22, 35, 36]. In the GemR cell lines, we expanded our study to include the CXCR1/2 antagonist Navarixin. This experiment elucidated trends of Gemcitabine increasing the CXCR1 axis expression along with CSC and EMT markers. Navarixin had varied responses for the expression, but in combination with Gemcitabine, there was a marked decrease in each of the markers examined. These data suggest that Navarixin works more effectively with the chemotherapy agent. We postulate this is due to the chemotherapy increasing the plasticity and sensitivity of the cells to a CXCR1-receptor blocking agent, which is necessary for its CSC-like state.

In further evaluation, we found increased co-expression of CSC markers with CXCR1 in the GemR cell lines, as found by CD44 and ALDH activity in IF and flow cytometry, respectively. In the flow cytometry experiment, we also found that Gem increased the frequency of ALDH+ cells in the GemR cells. However, with Navarixin treatment, that was negated back to control levels. Previous research supports that chemotherapy-resistant cells have higher expression of CSC markers [21], which we support in our research. We also found higher expression of CD44 in the GemR cell lines. In the literature, Chen et al. reported that chemoresistant PDAC tumor cells had upregulated CD44 and increased CD44 expression [37].

We expanded this research to an *in vivo* experiment with Nav, Gem, and combination experimental groups. The CD18-GemR cells were used for this experiment. The combination therapy with Navarixin and gemcitabine demonstrated superior antitumor and antimetastatic activity compared to either treatment alone (personal communication). We observed that Gem increased CXCL6 expression and decreased receptor expression. This is an expected result for the receptor-ligand relationship. The combination treatment provides an interesting result with almost no expression of either CXCR1 or CXCL6. This decrease in CXCR1 and CXCL6 is promising because it suggests that few cells can maintain this niche under the combination treatment, potentially decreasing the CSC-like cell population.

Overall, this study explores the CXCR1 axis as a potential target for decreasing the CSC-like phenotype of PDAC cells, thus allowing for more effective treatment of this deadly disease. These data suggest a role for CXCR1 in the CSC-like characteristics of PDAC and are linked with known CSC and EMT markers. The combination treatment shows a decrease in the expression of the CXCR1 axis. Together, our

data suggest the association of the CXCR1 axis with the CSC phenotype in PDAC.

Acknowledgements

This work was partly supported by grants R01CA228524, Cancer Center Support Grant (P30CA036727) from the National Cancer Institute, and National Institutes of Health (R.K.S.), and Caitlin Molczyk is supported by a T32CA009476 Eppley Institute Cancer Biology Training Grant from the National Cancer Institute. We thank Samuel M. and Janel L. Cohen, Distinguished Professorship of Pathology and Microbiology Fund (R.K.S.), for their generous support.

Disclosure of conflict of interest

None.

Address correspondence to: Dr. Rakesh K Singh, Department of Pathology, Microbiology, and Immunology, 985950 Nebraska Medical Center, Omaha, NE 68198-5900, USA. Tel: 402-559-9949; Fax: 402-559-5900; E-mail: rsingh@unmc.edu

References

[1] Siegel RL, Kratzer TB, Giaquinto AN, Sung H and Jemal A. Cancer statistics, 2025. CA Cancer J Clin 2025; 75: 10-45.

[2] Dzobo K, Senthebane DA, Ganz C, Thomford NE, Wonkam A and Dandara C. Advances in therapeutic targeting of cancer stem cells within the tumor microenvironment: an updated review. Cells 2020; 9: 1896-1934.

[3] Medema JP. Cancer stem cells: the challenges ahead. Nat Cell Biol 2013; 15: 338-344.

[4] Ramos EK, Hoffmann AD, Gerson SL and Liu H. New opportunities and challenges to defeat cancer stem cells. Trends Cancer 2017; 3: 780-796.

[5] Hermann PC and Sainz B Jr. Pancreatic cancer stem cells: a state or an entity? Semin Cancer Biol 2018; 53: 223-231.

[6] Lee CJ, Dosch J and Simeone DM. Pancreatic cancer stem cells. J Clin Oncol 2008; 26: 2806-2812.

[7] Kim WT and Ryu CJ. Cancer stem cell surface markers on normal stem cells. BMB Rep 2017; 50: 285-298.

[8] Grose R and Werner S. Wound healing studies in transgenic and knockout mice. A review. Methods Mol Med 2003; 78: 191-216.

[9] Singh S, Wu S, Varney M, Singh AP and Singh RK. CXCR1 and CXCR2 silencing modulates CXCL8-dependent endothelial cell proliferation, migration and capillary-like structure formation. Microvasc Res 2011; 82: 318-325.

[10] Ginestier C, Liu S, Diebel ME, Korkaya H, Luo M, Brown M, Wicinski J, Cabaud O, Charafe-Jauffret E, Birnbaum D, Guan JL, Dontu G and Wicha MS. CXCR1 blockade selectively targets human breast cancer stem cells in vitro and in xenografts. J Clin Invest 2010; 120: 485-497.

[11] Chen L, Fan J, Chen H, Meng Z, Chen Z, Wang P and Liu L. The IL-8/CXCR1 axis is associated with cancer stem cell-like properties and correlates with clinical prognosis in human pancreatic cancer cases. Sci Rep 2014; 4: 5911.

[12] Jiang J, Ye F, Yang X, Zong C, Gao L, Yang Y, Zhao Q, Han Z and Wei L. Peri-tumor associated fibroblasts promote intrahepatic metastasis of hepatocellular carcinoma by recruiting cancer stem cells. Cancer Lett 2017; 404: 19-28.

[13] Varney ML, Singh S, Li A, Mayer-Ezell R, Bond R and Singh RK. Small molecule antagonists for CXCR2 and CXCR1 inhibit human colon cancer liver metastases. Cancer Lett 2011; 300: 180-188.

[14] Sano M, Ijichi H, Takahashi R, Miyabayashi K, Fujiwara H, Yamada T, Kato H, Nakatsuka T, Tanaka Y, Tateishi K, Morishita Y, Moses HL, Isayama H and Koike K. Blocking CXCLs-CXCR2 axis in tumor-stromal interactions contributes to survival in a mouse model of pancreatic ductal adenocarcinoma through reduced cell invasion/migration and a shift of immune-inflammatory microenvironment. Oncogenesis 2019; 8: 8.

[15] Singh S, Nannuru KC, Sadanandam A, Varney ML and Singh RK. CXCR1 and CXCR2 enhances human melanoma tumourigenesis, growth and invasion. Br J Cancer 2009; 100: 1638-1646.

[16] Cheng Y, Ma XL, Wei YQ and Wei XW. Potential roles and targeted therapy of the CXCLs/CXCR2 axis in cancer and inflammatory diseases. Biochim Biophys Acta Rev Cancer 2019; 1871: 289-312.

[17] Raman D, Baugher PJ, Thu YM and Richmond A. Role of chemokines in tumor growth. Cancer Lett 2007; 256: 137-165.

[18] Fu S and Lin J. Blocking interleukin-6 and interleukin-8 signaling inhibits cell viability, colony-forming activity, and cell migration in human triple-negative breast cancer and pancreatic cancer cells. Anticancer Res 2018; 38: 6271-6279.

[19] Dabkeviciene D, Jonusiene V, Zitkute V, Zalyte E, Grigaitis P, Kirveliene V and Sasnauskiene A. The role of interleukin-8 (CXCL8) and CXCR2 in acquired chemoresistance of human colorectal carcinoma cells HCT116. Med Oncol 2015; 32: 258.

[20] Molczyk C and Singh RK. CXCR1: a cancer stem cell marker and therapeutic target in solid tumors. Biomedicines 2023; 11: 576.
[21] Sharma B, Varney ML, Saxena S, Wu L and Singh RK. Induction of CXCR2 ligands, stem cell-like phenotype, and metastasis in chemotherapy-resistant breast cancer cells. Cancer Lett 2016; 372: 192-200.
[22] Levina V, Marrangoni AM, DeMarco R, Gorelik E and Lokshin AE. Drug-selected human lung cancer stem cells: cytokine network, tumorigenic and metastatic properties. PLoS One 2008; 3: e3077.
[23] Ghallab AM, Eissa RA and El Tayebi HM. CXCR2 small-molecule antagonist combats chemoresistance and enhances immunotherapy in triple-negative breast cancer. Front Pharmacol 2022; 13: 862125.
[24] Graves DT and Jiang Y. Chemokines, a family of chemotactic cytokines. Crit Rev Oral Biol Med 1995; 6: 109-118.
[25] Proost P, Wuyts A and van Damme J. The role of chemokines in inflammation. Int J Clin Lab Res 1996; 26: 211-223.
[26] Richardson RM, Pridgen BC, Haribabu B, Ali H and Snyderman R. Differential cross-regulation of the human chemokine receptors CXCR1 and CXCR2. Evidence for time-dependent signal generation. J Biol Chem 1998; 273: 23830-23836.
[27] Zeilhofer HU and Schorr W. Role of interleukin-8 in neutrophil signaling. Curr Opin Hematol 2000; 7: 178-182.
[28] Rose JJ, Foley JF, Murphy PM and Venkatesan S. On the mechanism and significance of ligand-induced internalization of human neutrophil chemokine receptors CXCR1 and CXCR2. J Biol Chem 2004; 279: 24372-24386.
[29] Sturm A, Baumgart DC, d'Heureuse JH, Hotz A, Wiedenmann B and Dignass AU. CXCL8 modulates human intestinal epithelial cells through a CXCR1 dependent pathway. Cytokine 2005; 29: 42-48.
[30] Waugh DJ and Wilson C. The interleukin-8 pathway in cancer. Clin Cancer Res 2008; 14: 6735-6741.
[31] Nasser MW, Raghuwanshi SK, Grant DJ, Jala VR, Rajarathnam K and Richardson RM. Differential activation and regulation of CXCR1 and CXCR2 by CXCL8 monomer and dimer. J Immunol 2009; 183: 3425-3432.
[32] Raghuwanshi SK, Su Y, Singh V, Haynes K, Richmond A and Richardson RM. The chemokine receptors CXCR1 and CXCR2 couple to distinct G protein-coupled receptor kinases to mediate and regulate leukocyte functions. J Immunol 2012; 189: 2824-2832.
[33] Bajoghli B. Evolution and function of chemokine receptors in the immune system of lower vertebrates. Eur J Immunol 2013; 43: 1686-1692.
[34] Xu Q, Li R, Monte MM, Jiang Y, Nie P, Holland JW, Secombes CJ and Wang T. Sequence and expression analysis of rainbow trout CXCR2, CXCR3a and CXCR3b aids interpretation of lineage-specific conversion, loss and expansion of these receptors during vertebrate evolution. Dev Comp Immunol 2014; 45: 201-213.
[35] Brandolini L, Cristiano L, Fidoamore A, De Pizzol M, Di Giacomo E, Florio TM, Confalone G, Galante A, Cinque B, Benedetti E, Ruffini PA, Cifone MG, Giordano A, Alecci M, Allegretti M and Cimini A. Targeting CXCR1 on breast cancer stem cells: signaling pathways and clinical application modelling. Oncotarget 2015; 6: 43375-43394.
[36] Ha H, Debnath B and Neamati N. Role of the CXCL8-CXCR1/2 axis in cancer and inflammatory diseases. Theranostics 2017; 7: 1543-1588.
[37] Chen C, Zhao S, Zhao X, Cao L, Karnad A, Kumar AP and Freeman JW. Gemcitabine resistance of pancreatic cancer cells is mediated by IGF1R dependent upregulation of CD44 expression and isoform switching. Cell Death Dis 2022; 13: 682.